

MINERALOGY AND PETROLOGY OF THE HAM KIMBERLITE, SOMERSET ISLAND, NORTHWEST TERRITORIES

BRUCE C. JAGO AND ROGER H. MITCHELL

Department of Geology, Lakehead University, Thunder Bay, Ontario P7B 5E1

ABSTRACT

The Ham diatreme and dyke form separate fracture-controlled post-Silurian intrusive bodies in north-central Somerset Island, Northwest Territories, and consist of hypabyssal macrocrystalline serpentine-calcite kimberlite and kimberlite breccia. Alteration of previously consolidated kimberlite by fluids that deposited serpentine + calcite resulted in the development of modified kimberlites whose magnetic signature differentiates them from the unaltered varieties. Compositional data are provided for olivine, garnet and phlogopite macrocrystals. The spinel ranges in composition from aluminous magnesian chromite to magnesian ulvöspinel-magnetite. Serpentine exhibits extensive compositional variation; lizardite - 1T is developed in serpophitic segregations and retrograde olivine replacements, whereas lizardite - 6H occurs in prograde deuteric replacement and recrystallization. Ruby xenocrysts have been observed.

Keywords: kimberlite, magnetic expression, garnet, spinel, serpentine, ruby, Somerset Island, Northwest Territories.

SOMMAIRE

Le diatrème et le filon de Ham, dans la partie centre-nord de l'île de Somerset (Territoires du Nord-Ouest), ont été mis en place le long d'un système de fissures post-siluriennes. Ce sont des massifs hypabyssaux de kimberlite macrocristalline à serpentine et calcite, et de brèche kimberlitique. La kimberlite déjà consolidée, modifiée çà et là par des fluides saturés en serpentine et calcite, possède une signature magnétique qui la distingue de la roche saine. On établit la composition chimique de macrocristaux d'olivine, de grenat et de phlogopite. Le spinelle passe, en composition, d'une chromite alumineuse et magnésienne à un ulvöspinel-magnétite magnésien. La serpentine montre une grande variation dans sa composition; la lizardite-1T est présente dans les ségrégations serpophitiques et les pseudomorphoses rétrogrades d'olivine, tandis que la lizardite-6H est caractéristique de la serpentine de remplacement deutérique prograde et de recrystallisation. On trouve aussi du rubis en xénocristaux.

(Traduit par la Rédaction)

Mots-clés: kimberlite, expression magnétique, grenat, spinelle, serpentine, rubis, île de Somerset, Territoires du Nord-Ouest.

INTRODUCTION

The Ham diatreme and dyke, the most northerly known kimberlites of the Somerset Island kimberlite province (Mitchell 1976), are exposed as frost-heaved regolith within the headwaters of the Cunningham River in north-central Somerset Island, Northwest Territories (Fig. 1). The intrusive bodies occur in Ordovician limestone and are believed to be post-late Silurian in age, but to predate Cenozoic volcanic activity associated with Eurekan rifting (Mitchell 1975, Mitchell & Platt 1984).

FIELD RELATIONS

Figures 2 and 3 illustrate the geology and magnetic expression of the Ham diatreme and dyke. The flanks of the diatreme consist of highly magnetic (maximum 6800 γ above background) Type-1A kimberlite and enclose a weakly magnetic core (maximum 600 γ above background) of Type-1B and Type-2 kimberlite. The higher magnetic response of Type-1A kimberlite may be attributed to its relatively unaltered nature. In addition, Type-1A kimberlite contains a larger proportion of both primary, magnetic, iron-bearing oxides and secondary magnetite produced by serpentinization than does Type-2 kimberlite.

A roughly lenticular (75 \times 10 m) magnetic anomaly (maximum 400 γ above background) is associated with frost-heaved regolith above the Ham dyke. The symmetrical and uncomplicated nature of the anomaly, together with petrographic and field evidence, indicates that the Ham dyke is a vertical, uniformly magnetized, single-phase, unaltered intrusive body that is similar to the Ham diatreme of Type-1A kimberlite. Geophysical reconnaissance between the Ham diatreme and dyke does not indicate a near-surface link between the two bodies at the present level of erosion; therefore, age relations cannot be established.

Structural control of the diatreme and dyke in relation to two intersecting fractures can be inferred from Figure 2. The intersection of these two fractures (50° and 125°) coincides with the bulk of the Ham diatreme and a zone of intense alteration.

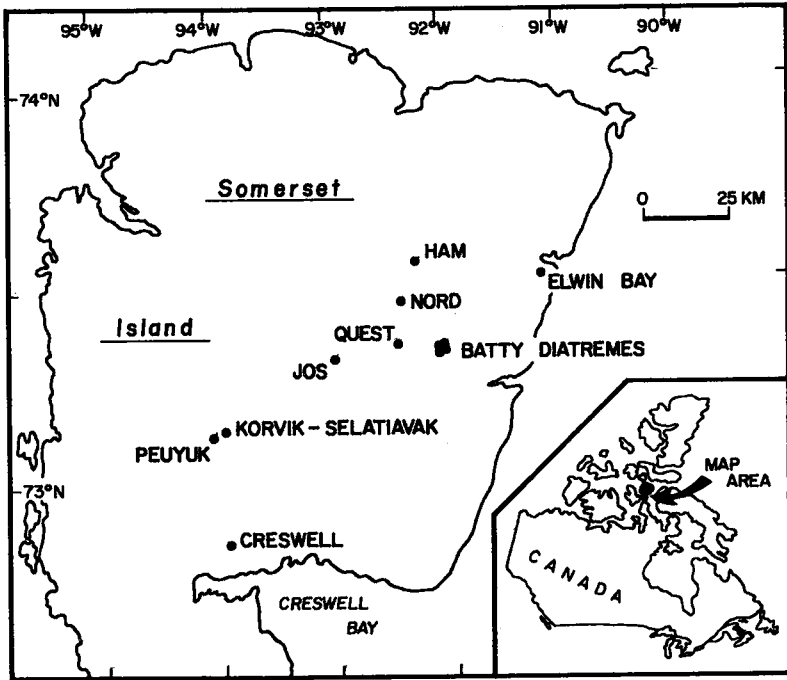


FIG. 1. Location map of the Somerset Island kimberlites.

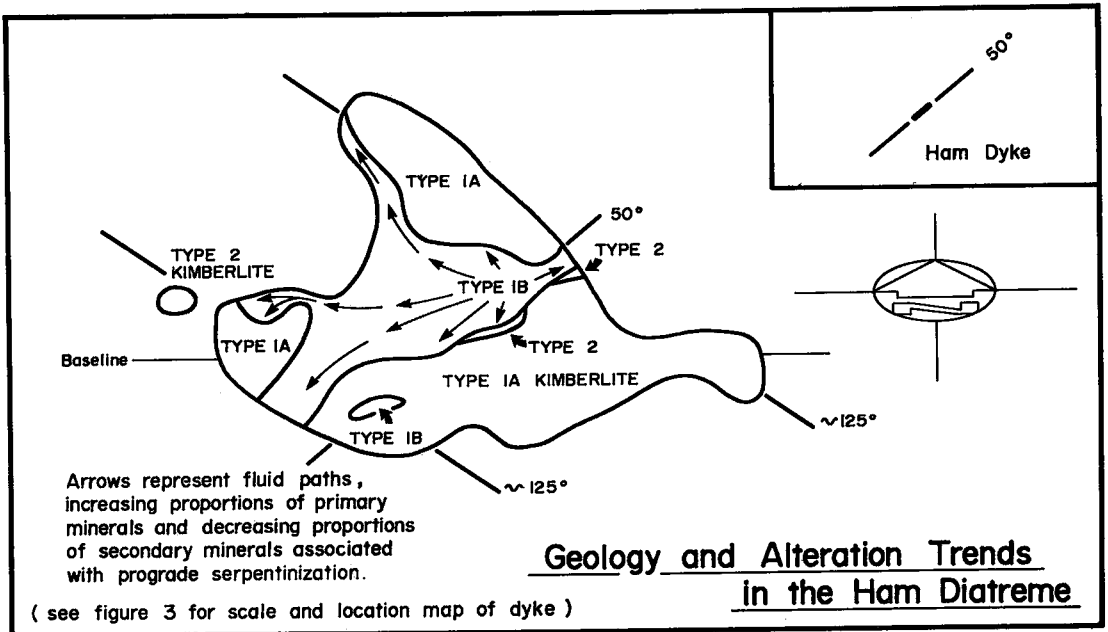


FIG. 2. Geology and alteration trends in the Ham diatreme.

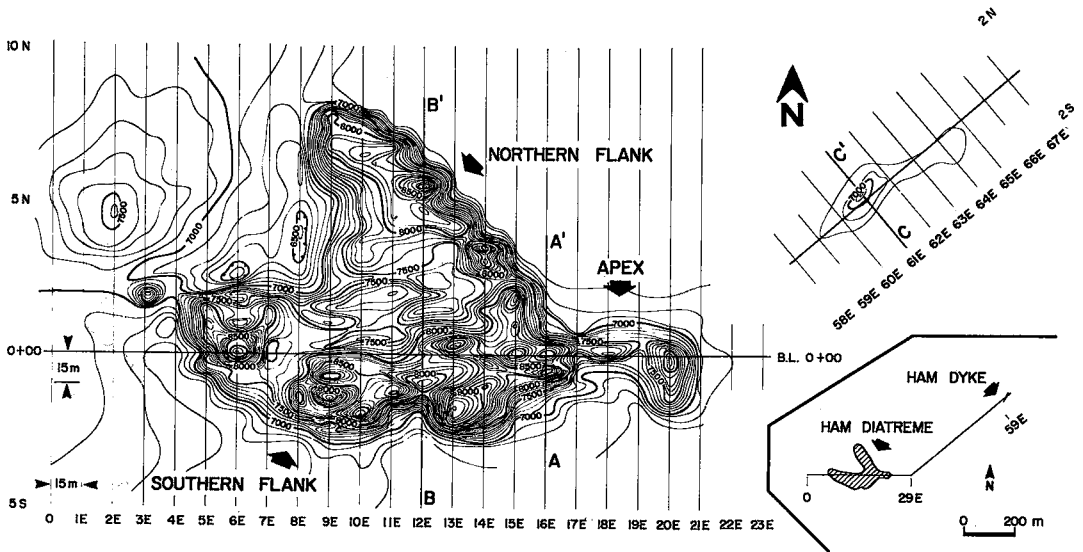


FIG. 3. Magnetic expression of the Ham diatreme and dyke.

Although no direct structural measurements of these fractures can be made, their presence is suggested by a) the linear coincidence of an elongate petroleum seep and the Ham dyke, both of which lie along a line trending 50° , and b) equal internal angles (75°) between fractures in broken limestone in the Cunningham River valley and the inferred flanks of the Ham diatreme. A comparison of Figures 2 and 3 shows that the pattern of the magnetic expression of a kimberlite, in areas of limited outcrop and where solifluction of regolith is active, is useful in determining the subcrop pattern of the kimberlite and relating its emplacement to regional structural features.

Structural controls of the emplacement of the Ham kimberlites are similar to those envisioned by Mitchell (1975) for the Peuyuk, Korvik and Selatiavak kimberlites and by Jago (1982) for the Batty Bay kimberlites. Mitchell (1975) interpreted the Central Somerset Island kimberlites to be enlarged fissure-fillings formed by a series of blows along three intersecting sets of fractures striking 50° , 125° and 175° . These fractures are recognizable on airphotos and were developed in Paleozoic sediments deposited on the flanks of the Precambrian Boothia granulite terrane, which is exposed in western Somerset Island. The fractures reflect structures generated in the basement and later reactivated during three phases of Cornwallis folding (Brown *et al.* 1969).

The complex magnetic expression of the Ham diatreme is similar to that of the multiphase Peuyuk kimberlite (Mitchell 1975). However, in the Peuyuk kimberlite, the higher magnetic response of Phase B compared to Phase C is attributed to the higher

content of primary magnetite in Phase B rather than to the complex history of alteration that has determined the magnetic expression of the Ham diatreme. The uniform nature of the magnetic expression of the Ham dyke is similar to that of the Korvik and Selatiavak kimberlites (Mitchell 1975) and the Inugapugsuk and Amayersuk kimberlites (Jago 1982) and reflects a relatively uniform distribution of magnetic iron-oxides in relatively unaltered single-phase kimberlite bodies.

PETROGRAPHY

The Ham diatreme (Fig. 2) is bell-shaped (270×165 m) and consists of three petrographically distinct varieties of kimberlite. Type-1A kimberlite forms the flanks and apex of the body and encloses Type-1B, which occupies the central portion of the diatreme and appears to cross-cut Type 1A in the northern and southern flanks. Type-2 kimberlite occurs as a discontinuous dyke within the diatreme and as a small circular body ten metres to the west. The Ham dyke is located 1.5 km to the northeast of the Ham diatreme. This northeast-southwest-oriented, lenticular intrusive body (*ca.* 75 m long) consists solely of a petrographic equivalent of Type-1A kimberlite.

Field relations and geophysical studies indicate that the Ham diatreme represents the root zone rather than the upper portion of a diatreme (Dawson 1967, Clement & Skinner 1979) and probably formed as a series of "blows" or enlarging fissure-intrusions along several intersecting set of fractures. These blows eventually coalesced to form a roughly bell-

shaped body. The Ham dyke represents a single, fissure-type intrusion which, at the present level of erosion, is separate from the Ham diatreme. Using the classification of Clement & Skinner (1979), the Ham dyke is a hypabyssal, macrocrystic, serpentine-carbonate kimberlite. The equivalent Type-1A kimberlite in the Ham diatreme (and highly altered Type-1B kimberlite) is a hypabyssal, macrocrystic, serpentine-carbonate kimberlite breccia; Type-2 kimberlite is a macrocrystic, carbonate-serpentine kimberlite.

Type-1A kimberlite is a black, massive to weakly foliated, macrocrystic rock containing two generations of olivine, phlogopite and spinel in a fine-grained groundmass of serpentine, carbonate, spinel, perovskite and apatite. Pyrope-garnet, chrome diopside and ruby were found in heavy-mineral separates. Carbonate forms tiny irregular veinlets, and serpentine and carbonate occur as round (Ham dyke) to cusp-shaped (Ham diatreme) segregations. Serpentine or carbonate (or both together) form partial to complete pseudomorphs after olivine and phlogopite. Limestone xenoliths are weakly to moderately altered and are flow-aligned parallel to intrusive contacts.

Type-1B kimberlite, a highly serpentinized and carbonated equivalent of Type-1A kimberlite, is a light reddish green, massive to porous rock containing highly altered limestone xenoliths and small (<3 mm long), massive to porous, oblong patches of serpentine or carbonate (or both). Two generations of olivine and spinel occur in a fine-grained groundmass of serpentine, carbonate, spinel and perovskite. Olivine is invariably replaced by secondary serpentine or carbonate (or both), and the spinel grains are extensively corroded.

Type-2 kimberlite is a massive, carbonate-rich, serpentine-poor, relatively unaltered equivalent of Type-1A kimberlite, in which first-generation phlogopite and second-generation spinel are scarce, and second-generation phlogopite is absent. Groundmass minerals include spinel, perovskite, carbonate and minor serpentine. Carbonate occurs as cusp-shaped segregations in the groundmass, whereas serpentine occurs in rare cross-cutting veins and as a rim on olivine.

MINERAL COMPOSITIONS

All minerals except garnet were analyzed at Purdue University using wavelength dispersion on a fully automated MAC 500 microprobe (Finger & Haddiacos 1972) and natural and synthetic standards. Raw X-ray counts were processed by the alpha-factor method of Bence & Albee (1968). Garnet was analyzed at Dalhousie University using energy dispersion on a Cambridge MKV microprobe with natural and synthetic standards. X-ray intensities were corrected with the EDATA2 program.

Olivine

Olivine occurs as small (<0.75 mm long), euhedral to subhedral microphenocrysts, and as large (<6 mm long), rounded anhedral strain-free and highly strained (xenolith-derived?) macrocrysts. Fresh microphenocrysts persist only in Type-2 kimberlite, and fresh macrocrysts and strained olivine only in Type-1A and Type-2 kimberlite.

Examination of Table 1 and Figures 4 and 5 shows that olivine macrocrysts and microphenocrysts cannot be distinguished by means of their forsterite content, and that both are forsterite-rich ($\text{Fo}_{93.5-89}$) compared to rounded, highly strained macrocrysts (Fo_{89-88}). Macrocrysts from Type-1A kimberlite exhibit a slightly narrower compositional range ($\text{Fo}_{92.5-91.5}$) than do macrocrysts and microphenocrysts from Type-2 kimberlite ($\text{Fo}_{93.5-89.5}$). Nickel-olivine contents are similar in both kimberlites (0.25–0 mol.% Ni_2SiO_4) and fall within the compositional range (0.40–0.05 mol.% Ni_2SiO_4) of deformed olivine. Both strain-free and deformed macrocrysts may be distinguished from microphenocrysts on the basis of lower contents of calcium (Table 1). Both macrocrysts and microphenocrysts are weakly zoned (approximately 1 mol.% Fo) toward an iron-rich and nickel-depleted (approximately 0.15 mol.% Ni-Ol) grain margin, although some crystals are not zoned, and some demonstrate reverse zoning.

Figure 6 shows that olivine in the Ham kimberlite is compositionally similar to olivine from other Somerset Island kimberlites (93.5–86.0 mol.% Fo) (Mitchell & Fritz 1973, Mitchell 1978a, 1979a), although the bimodal compositional variation demonstrated by macrocrysts and microphenocrysts from the Peuyuk (Mitchell & Fritz 1973), Tunraq (Mitchell 1979a) and Jos (Mitchell & Meyer 1980) kimberlites is not shared by olivine in the Ham or Elwin Bay (Mitchell 1979a) kimberlite (Fig. 6). The high content of magnesium in the Ham microphenocrysts (>90 mol.% Fo) compared to those from the Peuyuk and Tunraq kimberlites and the compositional overlap of macrocrysts and microphenocrysts may be ascribed to olivine crystalliza-

TABLE 1. REPRESENTATIVE COMPOSITIONS OF HAM OLIVINE

Oxide	1	2	3	4	5	6	7	8	9
SiO ₂	40.96	41.23	41.27	41.77	40.24	40.46	41.30	40.57	40.27
FeO*	7.46	6.98	8.23	7.48	10.75	10.79	6.85	8.43	9.84
MgO	51.23	51.65	50.07	50.57	48.37	48.11	51.68	49.92	49.72
CaO	0.05	0.02	0.02	0.00	0.04	0.03	0.09	0.09	0.09
MnO	0.00	0.00	0.02	0.12	0.00	0.05	0.00	0.00	0.00
NiO	0.29	0.13	0.07	0.15	0.08	0.12	0.17	0.20	0.20
Total	99.99100.01	99.68100.09	99.48	99.56100.09	99.21100.12				
Fo(mol%)	92.3	93.1	91.5	92.3	88.9	88.9	93.1	91.4	90.0

*Total Iron as FeO.

1-4 Olivine macrocrysts, Type-1A and Type-2 kimberlite.

5-6 Olivine porphyroclasts, Type-2 kimberlite.

7-9 Olivine microphenocrysts, Type-2 kimberlite.

tion from a magnesium-enriched magma, suggesting a batch mixing of magmas at depth. A similar origin is postulated for magnesium-rich microphenocrysts in the Elwin Bay (Mitchell 1978a) and Jos (Mitchell & Meyer 1980) kimberlites.

Garnet and chrome-diopside xenocrysts found in the Ham kimberlite indicate that olivine derived from the fragmentation of lherzolites is present. However, no chemical or textural criteria have been found to distinguish xenocrystic and liquidus olivine. The chemical similarity of these two paragenetic types is further complicated by the textural similarity of rounded strain-free olivine macrocrysts and rounded xenocrysts that do not exhibit porphyroclastic textures.

The range in olivine compositions and zonation trends observed in the Ham kimberlite is similar to that in olivine from South African and Greenland kimberlites. In general, olivine in kimberlite ranges from forsterite-rich (Fo_{93}) to relatively fayalite-rich (Fo_{86}) compositions (Mitchell 1973, Boyd & Clement 1977, Emeleus & Andrews 1975).

Mica

Two generations of phlogopite occur in the Ham diatreme and dyke; large (<5 mm across), rounded and corroded, anhedral macrocrysts and tiny (<0.1 mm long) euhedral, lath-shaped microphenocrysts. The macrocrysts are commonly broken, exhibit strained extinction and are pleochroic, light tan-brown to dark tan-brown to dark orange-brown in optically continuous crystals. A single corroded macrocryst exhibits a thin (<0.5 mm), corroded mantle of tan-brown phlogopite. Macrocrysts have been altered to septeclorite in Type-1B kimberlite but are relatively unaltered in all other phases. Microphenocrysts are inclusion- and strain-free and exhibit colorless to light-brown to tan-brown pleochroism. Crystals are commonly replaced by septeclorite in Type-1A and Type-1B kimberlite of the diatreme and contrast with only mildly corroded crystals in the Ham dyke. Microphenocrysts are absent in Type-1 kimberlite.

Low totals in the mica compositions (Table 2) reflect the partly chloritized nature of the mica. Macrocrysts are compositionally similar (Fig. 7) in the diatreme and dyke, although titanium and chromium contents in the diatreme (2.25–4.5 wt.% TiO_2 , 0–2.1 wt.% Cr_2O_3) have more restricted and broader ranges, respectively, than in the dyke (0.25–4.0 wt.% TiO_2 , 0.10–1.6 wt.% Cr_2O_3). Nickel contents (Fig. 8) are similar and vary from 0.04 to 0.26 wt.% NiO in diatreme macrocrysts and range up to 0.23 wt.% NiO in dyke macrocrysts. Individual crystals generally display weak normal and reverse zoning, respectively, in titanium and chromium contents.

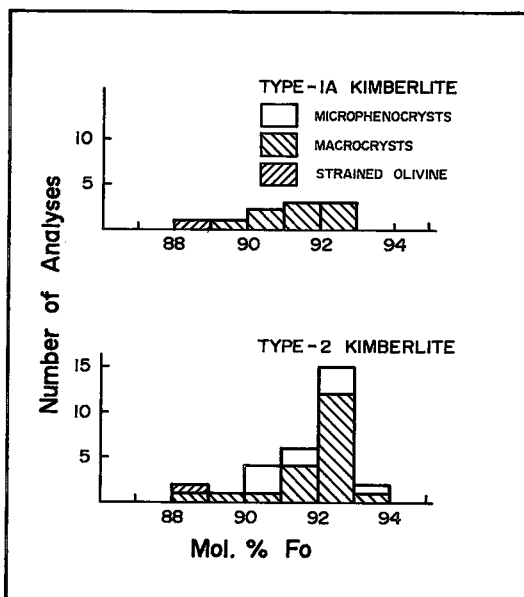


FIG. 4. Compositional variation (mol.% Fo) in olivine in the Ham kimberlites.

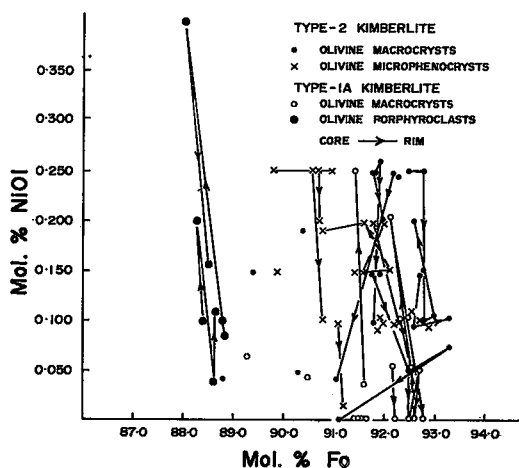


FIG. 5. Mol.% Ni-Ol versus mol.% Fo in olivine in the Ham kimberlites.

Figure 7 shows that the Ham macrocrysts are compositionally similar to mica in some other Somerset Island kimberlites, although Jos Type-B mica compositions (Mitchell & Meyer 1980) have a narrower range of chromium contents and Tunraq Ti-Cr-rich mica compositions (Mitchell 1979a) contain more titanium. Ham macrocrysts are titanium- and chromium-rich compared to macrocrysts at Elwin

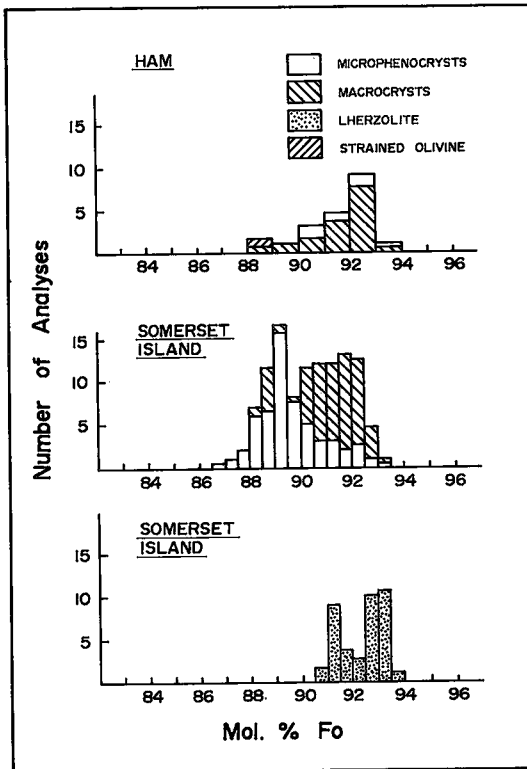


FIG. 6. Composition of olivine from the Ham kimberlite compared to that in other Somerset Island kimberlites.

Bay (Mitchell 1978a), Peuyuk (Mitchell 1975) and Jos (Type A; Mitchell & Meyer 1980).

The Ham macrocrysts lie outside the field of mica megacrysts of Dawson & Smith (1975), and several compositions with high contents of titanium and chromium plot in their field of secondary mica.

Microphenocrysts essentially are compositionally homogeneous, high-Ti (3.25 to 3.80 wt.% TiO₂), high-Cr (0.19 to 1.0 wt.% Cr₂O₃) phlogopite

[Mg/(Mg + Fe) 0.88 to 0.90]. These have a higher mean FeO content (4.89 wt.% FeO) than do Ham macrocrysts (3.79 wt.% FeO). Diatreme and dyke macrocrysts, respectively, have a higher mean TiO₂ content, and a higher Cr₂O₃ content for a given TiO₂ content than do microphenocrysts. Septechlorite pseudomorphs after diatreme microphenocrysts (Figs. 7, 8) are poor in titanium (0 to 0.38 wt.% TiO₂) and chromium (0 to 0.10 wt.% Cr₂O₃) and have correspondingly high Mg/(Mg + Fe) values compared to dyke microphenocrysts.

Compared to other occurrences of mica in the Somerset Island kimberlites (Figs. 7, 8), the Ham microphenocrysts are only similar to Jos Type-B macrocrysts (Mitchell & Meyer 1980) and contain higher titanium, chromium and nickel contents than Elwin Bay (Mitchell 1978a) or Jos (Mitchell & Meyer 1980) microphenocrysts. The Ham microphenocrysts are compositionally similar to the Mg-Ti-Cr-rich Type-II mica of Smith *et al.* (1978) but contain more chromium and less iron than their Type-I mica.

In contrast to mica compositions at Elwin Bay (Mitchell 1978a) and Tunraq (Mitchell 1979a), which evolved toward lower contents of titanium and chromium, phlogopite at Ham does not display any systematic compositional variation or chemical evolutionary trends. Also absent are complex mantling relationships, as exhibited by mica at Jos (Mitchell & Meyer 1980). Mitchell & Meyer attributed this relationship and the very broad range of Ti contents displayed by Jos Type-B mica to a crystal fractionation - magma mixing model. Smith *et al.* (1978) suggested that complex patterns of zoning are a result of the intrusion and mixing of a compositionally different magma into a hypabyssal magma-chamber immediately prior to the intrusion of the kimberlite and the onset of phenocryst crystallization. Such a process may be appropriate in explaining the compositional similarity between Ham megacrysts and microphenocrysts but cannot explain the absence of complex patterns of zoning in mica at Ham.

Garnet

Approximately 450 grains of orange, brown and deep red to purple garnet were recovered in mineral concentrates from the Ham diatreme and dyke. A detailed discussion of their compositional variation will be presented elsewhere (Jago & Mitchell, in prep.).

Compositionally, the garnet at Ham is chrome-pyrope (>0.5 wt.% Cr₂O₃; Dawson & Stephens 1975), and may be separated into a relatively Ti-rich, Cr-poor (megacryst trend) and a relatively Ti-poor, Cr-rich group (Iherzolite trend). The former group plots with Mitchell's (1979a) Ca-poor [Mg/(Mg + Fe) 0.76 to 0.88] suite from the Elwin

TABLE 2. REPRESENTATIVE COMPOSITIONS OF HAM MICA

Oxide	1	2	3	4	5	6	7	8	9
SiO ₂	39.05	39.52	36.97	36.02	39.32	40.71	36.94	37.33	23.45
TiO ₂	4.15	4.27	3.12	3.85	0.60	0.63	3.58	3.29	0.01
Al ₂ O ₃	13.48	12.89	13.96	16.00	12.08	11.96	12.75	12.69	13.46
Cr ₂ O ₃	1.07	1.16	0.61	0.69	0.85	0.91	0.91	1.06	0.02
FeO*	4.49	4.16	4.51	4.70	2.75	2.64	4.35	3.95	2.55
MgO	21.18	21.02	24.48	21.79	24.92	25.18	22.53	22.21	39.50
CaO	0.00	0.00	0.01	0.08	0.05	0.03	0.05	0.04	0.06
MnO	0.07	0.07	0.01	0.08	0.05	0.03	0.05	0.04	0.06
NiO	0.19	0.21	0.09	0.05	0.13	0.18	0.15	0.13	0.17
Na ₂ O	0.21	0.36	0.39	0.21	0.32	0.11	0.02	0.00	8.16
K ₂ O	10.27	9.36	6.66	8.34	8.75	8.96	7.33	6.77	0.38
Total	94.16	93.02	90.81	91.81	89.84	91.34	88.66	87.51	87.82

*Total iron as FeO.

1-2 Ham diatreme macrocrysts (core-rim)

3-4, 5-6 Ham dyke macrocrysts (core-rim)

7-8 Ham dyke microphenocrysts (core-rim)

9 Septechlorite replacing microphenocryst.

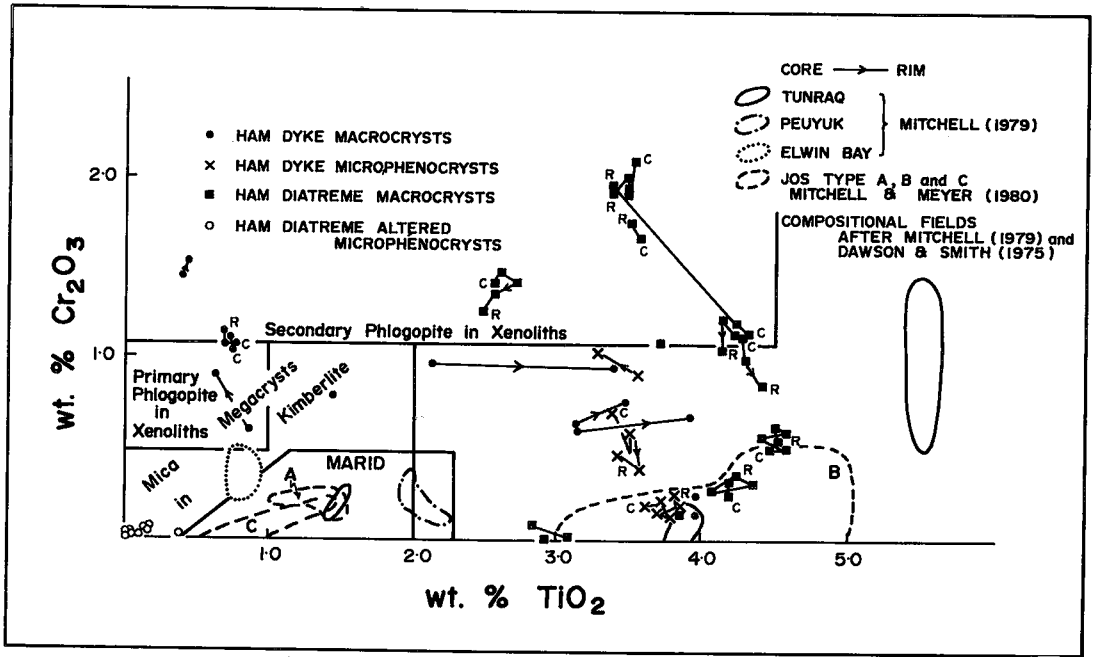


FIG. 7. Compositional variation (wt.% Cr_2O_3 versus wt.% TiO_2) of mica in the Ham kimberlites in comparison to compositional fields of mica from other kimberlites.

Bay (Mitchell 1978b) and Tunraq (Mitchell 1979a) kimberlites (Figs. 9, 10). These grains are larger than (> 1 cm diameter), and differ compositionally from garnet in garnet lherzolite xenoliths; they are believed to be true kimberlite phenocrysts (Mitchell 1979a). In contrast, the Ti-poor, Cr-rich garnet at Ham is compositionally similar (Figs. 9, 10) to garnet in lherzolite xenoliths from Elwin Bay (Mitchell 1978a) and other Somerset Island localities (Mitchell 1977) and is interpreted to be xenocrystic.

The composition of Ti-rich, Cr-poor garnet is similar (Figs. 9, 10) to that of the Cr-poor megacrysts of Boyd & Dawson (1972) from the Frank Smith and Monastery kimberlites, but is calcium-rich compared to the megacrysts of Reid & Hanor (1970) from Kimberley. Fe-poor, Ca-rich garnet in Lesotho granular garnet lherzolites (Boyd & Nixon 1975) plots with Ti-poor, Cr-rich garnet from Ham in Figures 9 and 10, both being slightly Fe-poor relative to the sheared garnet lherzolite suite of Boyd & Nixon (1975). All garnet compositions at Ham are magnesium-poor compared to garnet included in diamond (Meyer & Boyd 1970).

Garnet compositions at Ham fall into two major groups using the Dawson & Stephens (1975) statistical classification. The Ti-rich, Cr-poor macrocrysts belong to Group 1 (high-Ti, low-Cr titan-pyroxene), and Ti-poor, Cr-rich xenocrysts belong to Group 9 (low-Ti chrome-pyroxene) transitional toward low-Ca

chrome-pyroxene (Group 10) and titan-uvavovite-pyroxene (Group 11). Using the method of Danchin & Wyatt (1979), the garnet compositions are separated into Ti-poor peridotitic types (Groups 16 and 33) and Ti-rich peridotitic types (Groups 22, 26 and 37).

The larger proportion of xenocrysts over macrocrysts in the Ham diatreme relative to the Ham dyke reflects the higher xenolith content of the diatreme and a more violent history of intrusion, leading to xenolith fragmentation.

Clinopyroxene

Liquidus pyroxene is not found in the groundmass of the Ham kimberlites, but small, rounded, pitted and frosted, bottle-green crystals were recovered in mineral separates from the Ham diatreme. These crystals are similar in appearance to green clinopyroxene observed in garnet lherzolite xenoliths found only in the Ham diatreme.

Representative compositions of clinopyroxene are given in Table 3. According to the Stephens & Dawson (1977) classification (Table 3), 90% are chrome-diopside (Group 5, 0.21–2.81 wt.% Cr_2O_3), two grains are transitional between Cr-diopside and ureyitic diopside (Group 6), two are ureyitic diopside (1.72–6.15 wt.% Cr_2O_3) and the remaining two are diopside (Group 2, 0.13–0.99 wt.% Cr_2O_3).

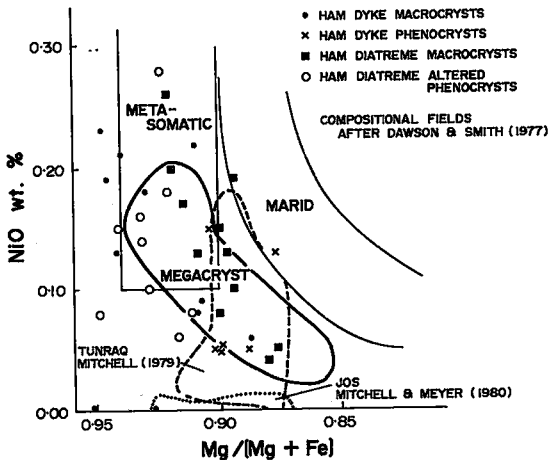


FIG. 8. NiO versus Mg/(Mg + Fe) in mica from the Ham kimberlites in comparison to compositional fields of mica from other kimberlites.

Pyroxene in Ham kimberlite concentrates is compositionally similar to clinopyroxene in garnet lherzolite xenoliths at Ham (Table 3, numbers 4 and 5) and Elwin Bay (Mitchell 1977, 1978b) and is undoubtedly of xenocrystic origin.

Spinel

The Ham diatreme and dyke contain two distinct spinel assemblages. Rounded, anhedral spinel crystallized prior to subhedral to euhedral spinel, which

typically occurs as discrete crystals or a euhedral mantle upon earlier-formed spinel. Four textural varieties can be discerned; these are: 1) rounded, aluminous magnesian chromite (AM-chromite), 2) euhedral to subhedral titaniferous magnesian aluminous chromite (titan-MA-chromite), 3) atoll spinel, and 4) euhedral, magnesium ulvöspinel - magnetite (MU-magnetite). Types 1, 2 and 3 are common to the diatreme and dyke, whereas Type 4 is found only in the dyke.

AM-chromite occurs as discrete, rounded and mildly corroded, transparent reddish-orange crystals up to 0.35 mm in diameter or as rounded crystals in the core of complexly zoned grains. Euhedral AM-chromite rarely is poikilitically enclosed in rounded olivine macrocrysts (Ham diatreme Type-1A kimberlite). These crystals and AM-chromite found as inclusions in pyrope in the Peuyuk kimberlite (Mitchell & Clarke 1976) are probably part of a high-pressure phenocrystic suite that formed at depth in the mantle.

Titan-MA-chromite and MU-magnetite occur as discrete, partially resorbed, euhedral to subhedral opaque groundmass crystals. The former are larger in the Ham dyke (0.30 mm maximum diameter) than in the diatreme (0.07 mm maximum diameter); the latter, found only in the Ham dyke, form crystals up to 0.1 mm in diameter. Both occur as solid solutions in a continuously zoned, partially resorbed, subhedral to euhedral mantle on earlier spinel phases. All spinel grains may be overgrown by a thin, spongy mantle of rutile-free, Ti-poor magnetite or a blocky, euhedral overgrowth of perovskite.

Atoll spinel, first described by Mitchell & Clarke (1976), is more abundant in the Ham dyke than in

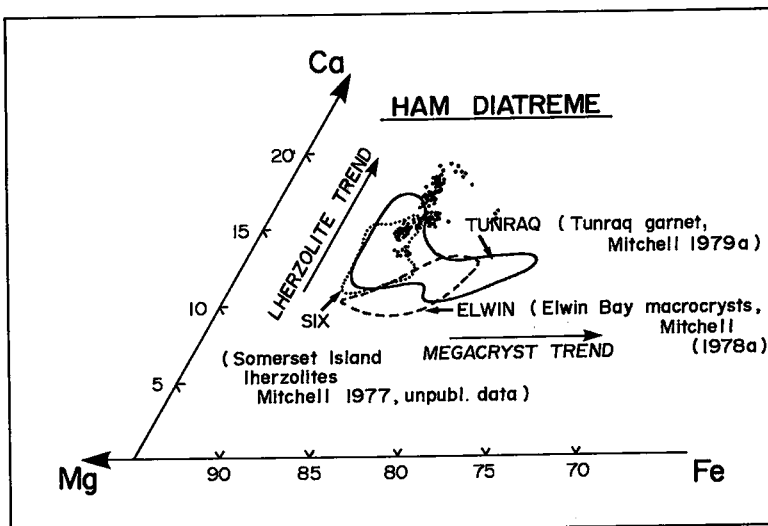


FIG. 9. Compositional variation (Ca-Fe-Mg plot) in garnet from the Ham diatreme in comparison to that from other kimberlites.

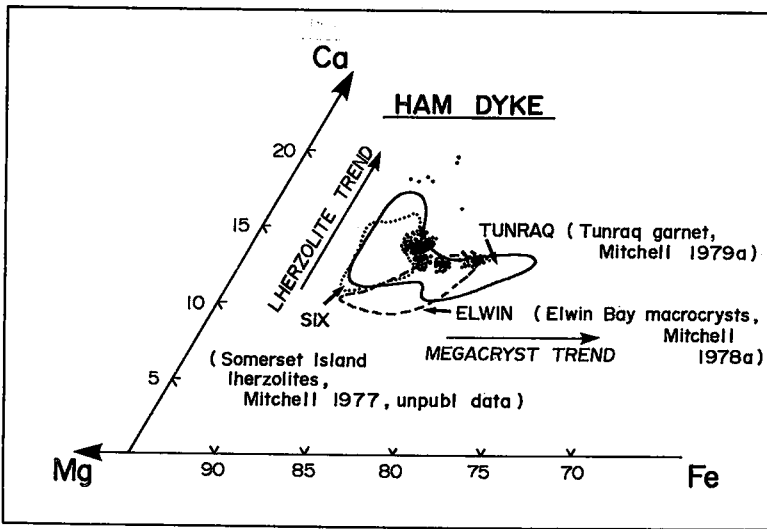


FIG. 10. Compositional variation (Ca-Fe-Mg plot) in garnet from the Ham dyke in comparison to that from other kimberlites.

the diatreme. Petrographic evidence suggests that this variety may have been obliterated in the Ham diatreme by extensive spinel-magma interaction prior to complete crystallization of the groundmass. Typically, an atoll spinel consists of a rounded core of AM-chromite or euhedral titan-MA-chromite overgrown by a continuously zoned mantle of titan-MA-chromite and MU-magnetite and an outer mantle of rutile-free, Ti-poor magnetite. Although the habit of the outer mantle appears to parallel that of the core spinel, core and mantle are separated by a thin, commonly discontinuous zone of silicate and carbonate similar in composition to the kimberlite groundmass. The irregular nature of the inner and outer contacts of this silicate zone suggest that it is related to spinel resorption (Mitchell & Clarke 1976).

Representative compositions are given in Table 4,

TABLE 3. REPRESENTATIVE COMPOSITIONS OF HAM CLINOPYROXENE

Oxide	1	2	3	4	5
SiO ₂	56.21	55.36	55.93	54.30	54.30
TiO ₂	0.26	0.16	0.57	0.28	0.45
Al ₂ O ₃	2.95	1.27	2.41	2.51	2.53
Cr ₂ O ₃	1.50	2.64	0.95	1.75	1.20
FeO*	2.79	1.87	3.72	2.51	3.60
MnO	0.08	0.09	0.13	0.09	0.13
MgO	17.07	16.53	17.65	16.98	18.33
CaO	17.03	20.95	17.40	18.80	17.68
Na ₂ O	2.07	1.63	1.39	1.92	1.43
K ₂ O	0.02	0.03	0.06	0.00	0.00
NiO	0.04	0.04	0.01	0.04	0.06
Total	100.02	100.57	100.22	99.18	99.71

Stephens & Dawson (1977) Classification

5 5 2 5 5

1-3 Clinopyroxene from mineral separates.
 4 Clinopyroxene from granular garnet lherzolite.
 5 Clinopyroxene from mosaic porphyroclastic garnet lherzolite.

and the compositional variation is illustrated in the "reduced" spinel prism (Haggerty 1973, Mitchell & Clarke 1976) in Figures 11 and 12. Spinel from the Ham diatreme varies from Al-rich, AM-chromite (Al-Mg-rich spinel) to titan-MA-chromite (Ti-bearing, Fe-Cr-rich spinel), reflecting a concomitant increase in the Cr/(Cr + Al) and Fe/(Fe + Mg) ratios of the kimberlite magma. Spinel in the Ham dyke ranges from AM-chromite to titan-MA-chromite to MU-magnetite (Fe³⁺-Ti-rich spinel). This evolutionary trend reflects initially a limited increase followed by a substantial decrease in the Cr/(Cr + Al) ratio at an approximately constant Fe/(Fe + Mg) ratio.

AM-chromite (Table 4, numbers 1-3) is compositionally similar in all phases of the Ham kimberlite (Figs. 11, 12), although that in Type-1A kimberlite, which is compositionally similar to highly aluminous chromite in the Peuyuk kimberlite (Mitchell & Clarke 1976) (Figs. 11, 12), evolved from much lower values of the Cr/(Cr + Al) ratio than AM-chromite in all other phases. The increasing Cr/(Cr + Al) ratio of these spinel compositions, which plot along the base of Figures 11 and 12, is attributed by Haggerty (1973) to their crystallization during a decrease in pressure as the evolving magma ascended from the mantle. The same type of spinel is found as inclusions in olivine and pyrope macrocrysts (Mitchell & Clarke 1976) and is probably a member of a high-pressure phenocrystic suite. The titanium content of the Ham AM-chromite (maximum 2.00 wt.% TiO₂) and aluminous chromite from other Somerset Island kimberlites (Jago 1982, Table 17A) is uniformly low in unzoned crystals; these plot near the base of the spinel prism.

TABLE 4. REPRESENTATIVE COMPOSITIONS OF HAM SPINEL

Oxide	1	2	3	4	5	6	7	8	9	10	11	12	13	14	15
TiO ₂	0.13	0.50	0.78	2.52	3.83	4.96	5.05	5.11	5.84	8.45	12.47	14.21	14.46	15.47	0.66
Al ₂ O ₃	34.57	12.38	12.29	14.28	13.90	17.38	9.12	11.50	7.34	8.73	7.21	7.18	8.80	7.63	0.37
Cr ₂ O ₃	30.85	56.21	55.73	46.54	42.98	33.68	44.82	39.98	43.88	0.20	0.00	0.00	0.68	1.42	0.08
FeO*	18.72	15.54	18.00	20.39	23.59	26.13	24.79	26.99	26.24	62.51	63.79	62.73	58.29	58.40	88.48
MnO	0.28	0.42	0.35	0.49	0.41	0.42	0.59	0.52	0.57	0.58	0.60	0.45	0.51	0.57	0.20
MgO	15.02	14.28	13.22	14.74	14.55	15.99	14.50	14.54	14.22	14.33	11.90	10.79	13.51	13.25	3.52
Total	99.57	99.33	100.37	98.96	99.26	98.56	98.87	98.64	98.09	94.80	95.97	95.36	96.25	96.74	93.31
Recalculated Analyses**															
Fe ₂ O ₃	4.88	3.87	4.08	7.82	9.58	13.31	10.77	12.77	11.66	46.31	43.04	38.38	37.30	36.09	65.55
FeO	14.33	12.06	14.33	13.35	14.97	14.16	15.10	15.50	15.75	20.84	25.06	28.20	24.72	25.92	29.49
Total	100.06	99.72	100.78	99.74	100.22	99.90	99.95	99.92	99.26	99.44	100.28	99.21	99.98	100.35	99.87
1-3 Aluminous magnesian chromite															
4-6 Titaniferous magnesian aluminous chromite															
7-9 Titaniferous magnesian chromite															
10-14 Magnesian ulvöspinel-ulvöspinel magnetite															
*Total iron expressed as FeO															
**Fe ₂ O ₃ and FeO calculated by methods of Carmichael (1967)															

The AM-chromite at Ham is compositionally similar to spinel in some ultrabasic xenoliths (Jago 1982, Table 17B), although in general, the latter group exhibits a greater range in Fe/(Fe + Mg) values. The presence of spinel lherzolite xenoliths in the Ham kimberlite regolith suggests that at least some AM-chromite may be of xenocrystic origin.

Relatively Ti-poor (2.00 wt.% TiO₂), Cr-rich, titan-MA-chromite (Table 4, numbers 4-6) was the first groundmass spinel to crystallize in all phases of the Ham kimberlites. These evolved *via* rare titan-magnesian-chromite (Table 4, numbers 7-9), at an approximately constant Fe/(Fe + Mg) ratio, toward Cr-poor, Ti-rich compositions (maximum 6.0 wt.% TiO₂). Textural and geochemical evidence suggests that spinel in Type-2 kimberlite did not evolve to

TiO₂ contents greater than approximately 3.0 wt.%. The trend toward enrichment in Ti and Fe³⁺ in the kimberlite magma and the crystallization of MUMagnetite (Table 4, numbers 10-14, maximum 16.6 wt.% TiO₂) have been discerned only in the Ham dyke. The last opaque phase to crystallize is magnetite poor in Ti, Al and Cr (Table 4, number 15).

Titanium-rich spinel in the Ham diatreme and compositionally similar spinel in the Peuyuk kimberlite (Mitchell & Clarke 1976) are enriched in MgAl₂O₄ compared to Ti-rich spinel in the Tunraq fissile micaceous kimberlite (Mitchell 1979a) and the Jos micaceous kimberlite (Mitchell & Meyer 1980). This suggests that spinel in kimberlite is generally richer in aluminum than spinel in micaceous kimberlite (Mitchell 1979a).

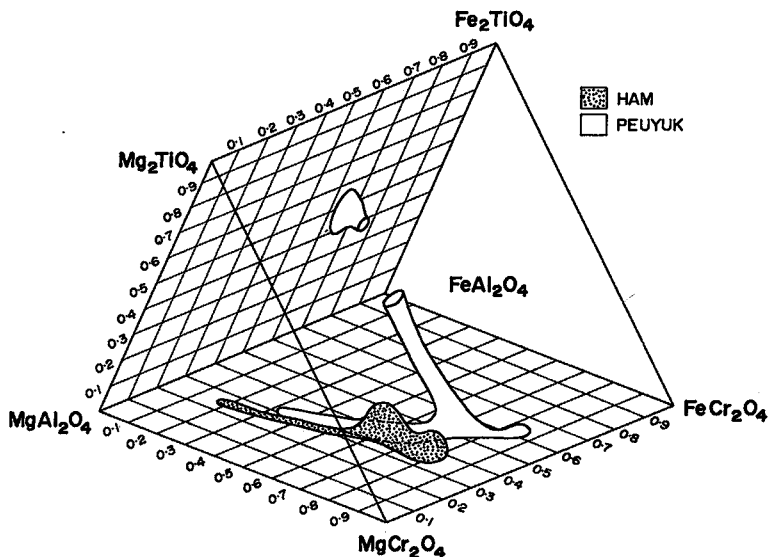


FIG. 11. Compositional fields of spinel from the Ham diatreme and Peuyuk (Mitchell & Clarke 1976) kimberlite.

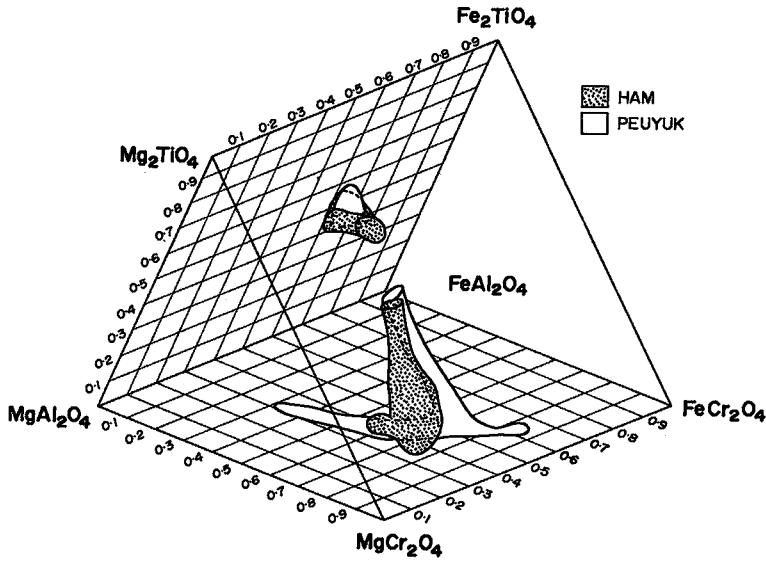


FIG. 12. Compositional fields of spinels from the Ham dyke and Peuyuk (Mitchell & Clarke 1976) kimberlite.

The initial similarity in spinel evolutionary trends for Type-1A and Type-1B kimberlite in the Ham diatreme and dyke suggests that a similar suite of spinel crystallized in each kimberlite. However, petrographic evidence suggests that extensive resorption of Ti-rich spinel occurred in the Ham diatreme subsequent to the stage of atoll-spinel development, obliterating evidence of extensive enrichment in Ti and Fe^{3+} .

Spinel evolutionary trends in the Ham kimberlites are similar, in general, to those determined for other kimberlites (Haggerty 1973, Mitchell & Clarke 1976, Mitchell 1978a, 1979a, Mitchell & Meyer 1980, Shee 1979, Pasteris 1983) in that enrichment in Fe^{3+} and Ti occurs as crystallization proceeds. The evolutionary trend toward the crystallization of MU-magnetite in the Ham and Peuyuk (Mitchell & Clarke 1976) kimberlites and in the Tunraq fissile micaceous kimberlite (Mitchell 1979a) is very similar (Figs. 11, 12; Mitchell 1979a, Fig. 9), although Figure 13 shows that the Tunraq spinel is depleted in aluminum as is the spinel in the highly evolved Jos micaceous kimberlite (Fig. 6, Mitchell & Meyer 1980). Neither of these kimberlites is known to have crystallized AM-chromite, in contrast to the Ham, Peuyuk (Mitchell & Clarke 1976) and Elwin Bay (Mitchell 1978a) kimberlites, all of which crystallized relatively Al-rich spinel.

Ruby

Eleven tiny (<0.10 mm across), transparent, pale

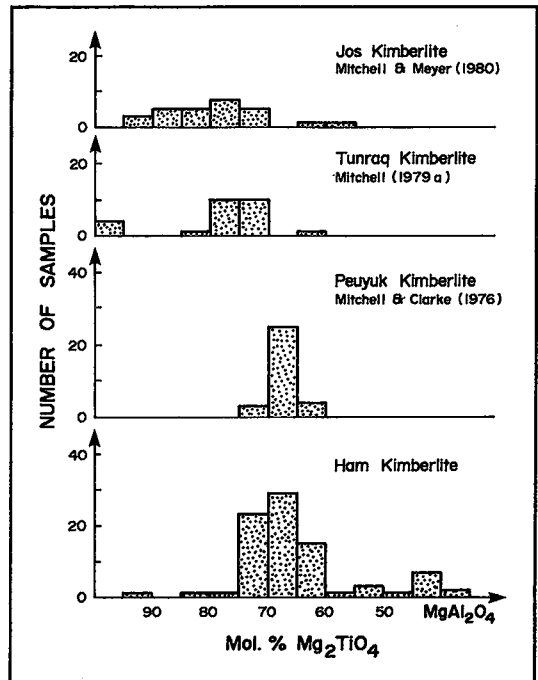


FIG. 13. Mol. % Mg_2TiO_4 variation in spinel from the Ham kimberlites compared to that from the Jos (Mitchell & Meyer 1980), Tunraq (Mitchell 1979a) and Peuyuk (Mitchell & Clarke 1976) kimberlites.

TABLE 5. REPRESENTATIVE COMPOSITIONS OF HAM RUBY

Oxide	1	2	3	4	5	6	7	8
SiO ₂	0.39	0.23	0.21	0.29	0.00	0.29	0.14	0.54
TiO ₂	0.00	0.00	0.00	0.00	0.00	0.09	0.00	0.00
Al ₂ O ₃	94.21	96.03	97.54	97.56	96.18	97.40	98.80	97.50
Cr ₂ O ₃	4.05	2.64	2.09	1.52	3.24	1.30	0.95	1.81
FeO*	0.38	0.29	0.29	0.23	0.64	0.22	0.01	0.03
MnO	0.06	0.01	0.04	0.00	0.00	0.01	0.00	0.00
MgO	0.02	0.02	0.01	0.02	0.19	0.13	0.02	0.03
CaO	0.02	0.01	0.02	0.01	0.00	0.02	-	-
Na ₂ O	0.00	0.06	0.03	0.04	-	-	-	-
K ₂ O	0.00	0.01	0.03	0.01	-	-	-	-
NiO	0.00	0.00	0.00	0.00	0.00	0.00	0.00	0.00
Total	99.13	99.30	100.26	99.68	100.25	99.46	99.92	99.91

*Total Iron as FeO.

1-4 Ham ruby

5 Secondary corundum in alkremite (Padovani & Tracy 1981)

6 Ruby inclusion in diamond (Meyer & Gübelin 1981).

7-8 Natural ruby (Deer et al. 1977)

pink, angular grains of ruby were recovered from mineral concentrates from the Type-1A kimberlite. Compositionally (Table 5, numbers 1-4), the ruby is aluminum-rich (97.56-94.21 wt.% Al₂O₃) and contains minor amounts of chromium (4.05-1.52 wt.% Cr₂O₃), iron (0.38-0.22 wt.% FeO) and silica (0.39-0.17 wt.% SiO₂). These compositions are similar in both major- and minor-element contents to secondary corundum in alkremites (pyrope garnet + Cr-poor spinel xenoliths; Table 5, number 5) and to ruby found as an inclusion in diamond (Table 5, number 6). Ruby from metamorphic terranes in the upper crust (Table 5, numbers 7-8) is compositionally distinct, containing more aluminum (99.80-97.50 wt.% Al₂O₃) and lower chromium (1.71-0.14 wt.% Cr₂O₃), iron (0.03-0 wt.% FeO) and silica (0.54-0 wt.% SiO₂).

The pressure of formation of ruby, estimated using the unit-cell parameters *a* 4.752 and *c* 12.989 Å and equations (2) and (3) of Finger & Hazen (1977), is between 3.3 and 3.6 kilobars.

The paragenesis of the ruby is uncertain. Ruby is commonly found in various upper-crust metamorphic terranes characterized by intrusion of alkaline magma into limestones (Wells 1956, Piat 1974). Less commonly it occurs as inclusions in diamond (Meyer & Gübelin 1981) and as a secondary mineral in corundum eclogite (Sobolev 1964, Shee 1978), alkremite (Padovani & Tracy 1981) and plagioclase-bearing metaperidotites (Lasnier 1974). Chemical data suggest that the ruby may have formed as a secondary mineral in a low-pressure environment. The absence of suitable parental, mantle-derived xenoliths suggests a metamorphic or contact-metasomatic origin. This is the second documented occurrence of ruby in Canada, the other being in stream sediments of the Tulameen River in British Columbia (Sinkankas 1959).

Carbonate

Primary carbonate occurs as tiny (<0.5 mm long), euhedral, inclusion-free, lath-shaped micropheno-

crysts (flow-aligned in the Ham dyke) and as coarse-grained, round to cusp-shaped, monomineralic segregations. Microphenocrysts have been wholly (Ham diatreme) to incipiently (Ham dyke) replaced by secondary carbonate or prograde serpentine during the alteration of the kimberlite groundmass.

Secondary carbonate occurs in two distinct parageneses. Carbonate veins (maximum length 3 cm), which occur predominantly in the Ham dyke and adjacent to the intrusive contacts of the Ham diatreme, are coarse-grained and inclusion-free, and commonly culminate in areas of locally pervasive carbonatization of the groundmass. These areas and bleached zones (maximum width 1 cm) adjacent to vein contacts are characterized by the replacement of pre-existing silicate and oxide minerals and a lightening in the color of the kimberlite groundmass. Carbonate pseudomorphs after olivine are restricted to Type-1B kimberlite. These consist of discrete, coarse, euhedral calcite crystals and crystals with successive epitaxial overgrowths, and are commonly altered and replaced by several generations of prograde serpentine.

Table 6 shows that the carbonate, regardless of paragenesis, is calcite. Lath-shaped crystals and segregations of primary carbonate crystallized as a residual phase in the Ham kimberlites. Textural (*e.g.*, Jago 1982, Mitchell 1979b) and experimental (*e.g.*, Franz & Wyllie 1967, Ferguson & Currie 1971) evidence indicates that these are primary structures and that they may be related to liquid immiscibility.

Serpentine

Primary serpentine consists of iron-poor (Table 7, numbers 1-2), pale yellow to pale brown "spherulitic lizardite" (Wicks *et al.* 1977) forming discrete, round (diameter 0.5 mm) to cusped segregations. The margin of these structures is mildly corroded and intergrown with pale yellow groundmass serpentine (lizardite-1T; Mitchell, unpubl. microdiffraction data). Monomineralic segregations are common only in Type-1A kimberlite, being replaced by secondary carbonate and prograde serpentine in Type-1B kimberlite. Primary serpentine in Type-2 kimberlite con-

TABLE 6. REPRESENTATIVE COMPOSITIONS OF HAM CARBONATE

Oxide	1	2	3	4	5
MnO	0.00	0.01	0.13	0.00	0.00
FeO*	0.10	0.04	0.24	0.11	0.13
MgO	0.37	0.32	0.36	0.45	0.49
CaO	59.40	58.72	58.46	59.46	59.44
Total	59.87	59.09	59.19	60.02	60.06

*Total Iron as FeO.

1 Carbonate segregation

2 Carbonate in serpentine segregation

3 Carbonate replacing olivine

4 Euhedral carbonate in serpentine replacing olivine

5 Euhedral carbonate lath in Ham dyke groundmass

TABLE 7. REPRESENTATIVE COMPOSITIONS OF HAM SERPENTINE AND ASSOCIATED OPAQUE MINERALS

Oxide	1	2	3	4	5	6	7	8	9**
SiO ₂	41.32	40.67	40.41	39.80	42.65	39.79	39.20	38.43	-
TiO ₂	0.00	0.00	0.01	0.03	0.01	0.05	0.09	0.38	0.12
Al ₂ O ₃	0.74	1.07	0.32	0.41	0.21	0.21	0.46	1.25	0.00
Cr ₂ O ₃	0.00	0.04	0.06	0.06	0.04	0.07	0.00	0.06	0.00
FeO*	2.09	2.45	6.32	8.59	9.11	12.23	6.20	5.78	86.07
MgO	40.23	39.23	35.93	33.85	33.17	30.55	34.01	36.27	0.81
CaO	0.01	0.05	0.09	0.07	0.22	0.31	0.25	0.11	-
MnO	0.00	0.00	0.07	0.08	0.14	0.14	0.09	0.11	2.17
NiO	0.00	0.00	0.18	0.11	0.32	0.57	0.04	0.17	-
Na ₂ O	0.00	0.00	0.00	0.00	0.00	0.00	0.00	0.09	-
K ₂ O	0.01	0.00	0.07	0.05	0.02	0.00	0.01	0.07	-
Total	84.40	83.51	83.46	83.05	85.89	83.92	80.35	82.72	89.17
Fe/(Fe+Mg)	0.028	0.033	0.089	0.124	0.133	0.183	0.093	0.080	-

*Total Iron as FeO

**Low total due to Iron calculated as FeO and small crystal size.

1-2 Serpentine segregation.

3-4 3 serpentine beside fresh olivine, 4 serpentine at grain margin.

5-6 5 serpentine at vein margin, 6 in vein core.

7-8 Core/margin pair in non-pseudomorphous serpentine Type-1B kimberlite.

9 Magnetite in serpentine.

sists solely of pale yellow, groundmass serpentine (lizardite-1T; Mitchell, unpubl. microdiffraction data).

Secondary serpentine occurs in "retrograde and prograde pseudomorph and nonpseudomorph" assemblages (Wicks *et al.* 1977), respectively. Retrograde serpentinization, characterized by lizardite-1T pseudomorphs after olivine, occurred after the crystallization of the kimberlite groundmass and primary serpentine but before the onset of carbonate metasomatism and prograde serpentinization. Olivine grains in Type-1A and Type-2 kimberlite are wholly to partly replaced by "coarse-bladed" lizardite forming "hour-glass" structures and medium- to fine-grained lizardite veins and "mesh rims and mesh centres". Serpentine in partial pseudomorphs and in veins adjacent to fresh olivine is brown-yellow, grading to orange-yellow at grain margins and in veins cores. Geochemical evidence (Jago 1982, Wicks *et al.* 1977) indicates that this color variation is due to iron expulsion from the advancing front of serpentinization against fresh olivine (Table 7, numbers 3, 5) toward the margin of grains (Table 7, number 4) and the core of veins (Table 7, number 6). At these sites, iron crystallizes as irregular masses of magnetite (Table 7, number 9) and as fine dustings or discrete crystals of magnetite, respectively. The trend toward the depletion of iron from serpentine at the advancing front of serpentinization and its enrichment at the margin of grains is paralleled by a decrease in the silica content of the pseudomorph away from the advancing front of serpentinization (Table 7, *e.g.*, numbers 3, 5). In this manner, the silica content of retrograde serpentine decreases with an increase in the degree of serpentinization, a process that is reversed during prograde serpentinization (Jago 1982, Golightly & Arancibia 1979). The thermal stability of lizardite

(Caruso & Chernosky 1979) constrains retrograde serpentinization to temperatures below approximately 490°C.

Prograde nonpseudomorphous serpentine (Wicks *et al.* 1977) characterizes Type-1B kimberlite. This is dominated by the extensive recrystallization of primary and retrograde assemblages to very fine-grained, pale yellow, mosaic-type, multilayer, lizardite-6H (Mitchell, unpubl. microdiffraction data), and the development of antigorite in the groundmass. Chrysotile is scarce or absent, suggesting a hydrous environment (Wicks & Plant 1979) and reinforcing earlier suggestions that Type-1B kimberlite is coincident with a zone of prolonged circulation of fluid and elevated temperatures. Experimental data indicate that temperatures during this prograde event did not exceed approximately 500°C (Caruso & Chernosky 1979). Nonpseudomorphous serpentine is relatively iron-poor (Table 7, numbers 7, 8), with moderately high contents of silica (Jago 1982, Golightly & Arancibia 1979). Coarse crystals of magnetite commonly are found in the groundmass adjacent to relict pseudomorphs. Prograde serpentine assemblages are absent in the Ham dyke, where secondary mineral assemblages consist solely of rare carbonate veins and retrograde serpentine.

Figure 2 illustrates the distribution of petrographic types of kimberlite in the Ham diatreme and inferred paths of fluid, and, thus, the structural control of alteration assemblages. Type-1A and Type-2 kimberlite are characterized by primary carbonate and primary and retrograde serpentine. Type-1B kimberlite is characterized by intense carbonatization and prograde serpentine assemblages; the latter replaces primary and retrograde serpentine and primary and secondary carbonate. Arrows, representing paths of fluid, emanate from the area of intersection of the north- and south-limb fractures and illustrate the direction of increasing proportions of primary minerals and decreasing proportions of secondary carbonate and prograde serpentine. Petrographic evidence shows that the contact between Type-1A and Type-1B kimberlite is characterized by a gradually increasing proportion of secondary minerals and that Type-1B kimberlite is a highly altered equivalent of Type-1A.

Very little definitive work has been done on the serpentine mineralogy of kimberlite or the process of serpentinization in kimberlite. This study shows that primary and retrograde serpentine formed during and after the final stages of groundmass crystallization, respectively, but also that these assemblages can be obliterated by late-stage circulation of fluids, leading to prograde serpentinization. Several investigations of the mineralogy of serpentine in kimberlite have been attempted (*e.g.*, McCallum *et al.* 1975, Emeleus & Andrews 1975, Pasteris 1983, Mitchell 1978a) but, owing to the complex nature of the ser-

pentinization process, are inadequate to describe fully the serpentine parageneses.

SUMMARY

The Ham diatreme and dyke are hypabyssal, macrocrystic, serpentine-carbonate kimberlite (dyke) to kimberlite breccia (diatreme) (Clement & Skinner 1979) belonging to the least-evolved type of Mitchell's (1979b) kimberlite clan. Initially, the kimberlite magma crystallized garnet and olivine and rare aluminum-rich AM-chromite. As the magma ascended and pressure decreased, olivine continued to crystallize, but garnet ceased to be a liquidus phase, its place being taken by increasing amounts of AM-chromite (evolving to more Cr-rich compositions) and by later crystallizing Ti- and Cr-rich phlogopite.

Intrusion of the Ham diatreme (Type-1A kimberlite) probably occurred as a series of "blows" along a set of intersecting fractures. These "blows" eventually coalesced to form the present intrusive body. Whether the single intrusive event that formed the Ham dyke was contemporaneous or not with the formation of the Ham diatreme is unknown.

Olivine, phlogopite and spinel crystallized as postintrusion microphenocrysts, followed by later-crystallizing perovskite, apatite, carbonate and serpentine, which formed the groundmass. Spinel crystallized as discrete grains and mantles upon pre-existing spinel grains and evolved from Ti-bearing, Fe²⁺-Cr-rich titan-MA-chromite to Ti-Fe³⁺-rich MU-magnetite at an approximately constant Fe/(Fe + Mg) ratio. These were replaced by Ti-free magnetite, which crystallized epitactically upon a core of earlier spinel. Although atoll spinel is believed to have formed in both the Ham diatreme and dyke, it is only preserved in the Ham dyke. As crystallization proceeded, late-stage volatile-rich fluids separated and eventually crystallized as segregation textures. Olivine, mica, spinel and apatite ceased to be liquidus phases as the serpentine-carbonate groundmass crystallized. Prograde serpentinization followed final crystallization of the groundmass and, in the Ham diatreme, was followed by a period of higher temperatures and deuteric alteration leading to the formation, by carbonatization and serpentinization, of Type-1B kimberlite.

ACKNOWLEDGEMENTS

This study was supported by the Natural Sciences and Engineering Research Council of Canada (NSERC). Logistical support in the Arctic was provided by the Polar Continental Shelf Project of the Department of Energy, Mines and Resources,

Canada. Valerie Dennison is thanked for field assistance. Bruce Jago sincerely wishes to thank Dr. Mitchell for encouraging the original M.Sc. study, which was supported by an NSERC graduate fellowship.

REFERENCES

- BENCE, A.E. & ALBEE, A.L. (1968): Empirical correction factors for the electron microanalysis of silicates and oxides. *J. Geol.* **76**, 382-403.
- BOYD, F.R. & CLEMENT, C.R. (1977): Compositional zoning of olivines in kimberlite from the De Beers mine, Kimberley, South Africa. *Carnegie Inst. Wash. Year Book* **76**, 485-493.
- _____ & DAWSON, J.B. (1972): Kimberlite garnets and pyroxene-ilmenite intergrowths. *Carnegie Inst. Wash. Year Book* **71**, 373-378.
- _____ & NIXON, P.H. (1975): Origins of ultramafic nodules from some kimberlites of northern Lesotho and the Monastery mine, South Africa. *Phys. Chem. Earth* **9**, 431-454.
- BROWN, R.J., DALZIEL, I.W.D. & RUST, B.R. (1969): The structure, metamorphism and development of the Boothia Arch, Arctic Canada. *Can. J. Earth Sci.* **6**, 525-543.
- CARMICHAEL, I.S.E. (1967): The iron-titanium oxides of salic volcanic rocks and their associated ferromagnesian silicates. *Contr. Mineral. Petrology* **14**, 36-64.
- CARUSO, L.J. & CHERNOSKY, J.V., JR. (1979): The stability of lizardite. *Can. Mineral.* **17**, 757-769.
- CLEMENT, C.R. & SKINNER, E.M.W. (1979). A textural-genetic classification of kimberlite rocks. *Cambridge Kimberlite Symposium II, Chairman's Summaries and Poster Session Abstr.*, 19-21.
- DANCHIN, R.V. & WYATT, B.A. (1979): Statistical cluster analysis of garnets from kimberlites and their xenoliths. *Cambridge Kimberlite Symposium II, Chairman's Summaries and Poster Session Abstr.*, 22-27.
- DAWSON, J.B. (1967): A review of the geology of kimberlite. In *Ultramafic and Related Rocks* (P.J. Wyllie, ed.). J. Wiley & Sons, New York.
- _____ & SMITH, J.V. (1975): Chemistry and origin of phlogopite megacrysts in kimberlite. *Nature* **253**, 336-338.
- _____ & _____ (1977): The MARID (mica-amphibole-rutile-ilmenite-diopside) suite of xenoliths in kimberlite. *Geochim. Cosmochim. Acta* **41**, 309-323.

- _____ & STEPHENS, W.E. (1975): Statistical classification of garnets from kimberlite and associated xenoliths. *J. Geol.* **83**, 589-607.
- DEER, W.A., HOWIE, R.A. & ZUSSMAN, J. (1977): *An Introduction to the Rock-Forming Minerals*. Longman, London.
- EMELEUS, C.H. & ANDREWS, J.R. (1975): Mineralogy and petrology of kimberlite dyke and sheet intrusions and included peridotite xenoliths from southwest Greenland. *Phys. Chem. Earth* **9**, 179-197.
- FERGUSON, J. & CURRIE, K.L. (1971): Evidence of liquid immiscibility in alkaline ultrabasic dikes at Callander Bay, Ontario. *J. Petrology* **12**, 561-585.
- FINGER, L.W. & HADIDIACOS, C.G. (1972): Electron microprobe automation. *Carnegie Inst. Wash. Year Book* **71**, 598-600.
- _____ & HAZEN, R.M. (1977): Crystal structure and compressibility of ruby to 80 Kbar. *Carnegie Inst. Wash. Year Book* **76**, 525-527.
- FRANZ, G.W. & WYLLIE, P.J. (1967): Experimental studies in the system CaO-MgO-SiO₂-CO₂-H₂O. In *Ultramafic and Related Rocks* (P.J. Wyllie, ed.). J. Wiley & Sons, New York.
- GOLIGHTLY, J.P. & ARANCIBIA, O.N. (1979): The chemical composition and infrared spectrum of nickel- and iron-substituted serpentine from a nickeliferous laterite profile, Soroaka, Indonesia. *Can. Mineral.* **17**, 719-728.
- HAGGERTY, S.E. (1973): Spinels of unique composition associated with ilmenite reactions in the Lihobong kimberlite pipe, Lesotho. In *Lesotho Kimberlites* (P.H. Nixon, ed.). Lesotho National Development Corp., Maseru, Lesotho.
- JAGO, B.C. (1982): *The Mineralogy and Petrology of the Ham Kimberlite, Somerset Island, N.W.T., Canada*. M.Sc. thesis, Lakehead Univ., Thunder Bay, Ont.
- LASNIER, B. (1974): Origine du corindon secondaire dans les gabbros, norites et pyroxénolites à spinelle du Pont de Lowen. *Soc. Géol. Minéral. Bretagne, Bull.* **6**, 109-130.
- MCCALLUM, M.E., EGGLEER, D.H. & BURNS, L.K. (1975): Kimberlitic diatremes in northern Colorado and southern Wyoming. *Phys. Chem. Earth* **9**, 149-161.
- MEYER, H.O.A. & BOYD, F.R. (1970): Inclusions in diamonds. *Carnegie Inst. Wash. Year Book* **68**, 315-320.
- _____ & GÜBELIN, E. (1981): Ruby in diamond. *Gems Gemology* **17**, 153-156.
- MITCHELL, R.H. (1973): Composition of olivine, silica activity and oxygen fugacity in kimberlite. *Lithos* **6**, 65-81.
- _____ (1975): Geology, magnetic expression, and structural control of the central Somerset Island kimberlites. *Can. J. Earth Sci.* **12**, 757-764.
- _____ (1976): Kimberlites of Somerset Island, District of Franklin. *Geol. Surv. Can. Pap.* **76-1A**, 501-502.
- _____ (1977): Ultramafic xenoliths from the Elwin Bay kimberlite: the first Canadian paleogeotherm. *Can. J. Earth Sci.* **14**, 1202-1210.
- _____ (1978a): Mineralogy of the Elwin Bay kimberlite, Somerset Island, N.W.T., Canada. *Amer. Mineral.* **63**, 47-57.
- _____ (1978b): Garnet lherzolites from Somerset Island, Canada and aspects of the nature of perturbed geotherms. *Contr. Mineral. Petrology* **67**, 341-347.
- _____ (1979a): Mineralogy of the Tunraq kimberlite, Somerset Island, N.W.T., Canada. In *Kimberlites, Diatremes and Diamonds: Their Geology, Petrology and Geochemistry* (F.R. Boyd & H.O.A. Meyer, eds.). *Amer. Geophys. Union, Proc. Second Int. Kimberlite Conf., Spec. Pap.* **SP0024**, 161-171.
- _____ (1979b): The alleged kimberlite-carbonatite relationship: additional contrary mineralogical evidence. *Amer. J. Sci.* **279**, 570-589.
- _____ & CLARKE, D.B. (1976): Oxide and sulphide mineralogy of the Peuyuk kimberlite, Somerset Island, N.W.T., Canada. *Contr. Mineral. Petrology* **56**, 157-172.
- _____ & FRITZ, P. (1973): Kimberlite from Somerset Island, District of Franklin, N.W.T. *Can. J. Earth Sci.* **10**, 384-393.
- _____ & MEYER, H.O.A. (1980): Mineralogy of micaceous kimberlite from the Jos dyke, Somerset Island, N.W.T. *Can. Mineral.* **18**, 241-250.
- _____ & PLATT, R.G. (1984): The Freemans Cove volcanic suite: field relations, petrochemistry and tectonic setting of nephelinite-basanite volcanism associated with rifting in the Canadian Arctic Archipelago. *Can. J. Earth Sci.* **21**, 428-436.
- PADOVANI, E.R. & TRACY, R.J. (1981): A pyrope-spinel (alkremite) xenolith from Moses Rock dike: first known North American occurrence. *Amer. Mineral.* **66**, 741-745.
- PASTERIS, J.D. (1983): Spinel zonation in the De Beers kimberlite, South Africa: possible role of phlogopite. *Can. Mineral.* **21**, 41-58.
- PIAT, D. (1974): Le rubis himalayen d'Hunza. *Assoc. franç. Gemmologie, Bull.* **41**, 5.

- REID, A.M. & HANOR, J.S. (1970): Pyrope in kimberlite. *Amer. Mineral.* **55**, 1374-1379.
- RUCKLIDGE, J. (1967): A computer program for processing microprobe data. *J. Geol.* **75**, 126.
- SHEE, S.R. (1978): *The Mineral Chemistry of Xenoliths from the Orapa Kimberlite Pipe, Botswana*. M.Sc. thesis, Univ. Cape Town, Cape Town, South Africa.
- _____ (1979): The opaque oxides of the Wesselton mine. *Cambridge Kimberlite Symposium II, Chairman's Summaries and Poster Session Abstr.*, 54-59.
- SINKANKAS, J. (1959): *Gemstones of North America*. D. Van Nostrand and Co., New York.
- SMITH, J.V., BRENNESHOLTZ, R. & DAWSON, J.B. (1978): Chemistry of micas from kimberlites and xenoliths. I. Micaceous kimberlites. *Geochim. Cosmochim. Acta* **42**, 959-971.
- SOBOLEV, N.V. (1964): Xenolith of eclogite with ruby. *Dokl. Acad. Sci. USSR, Earth Sci. Sect.* **157**, 112-114.
- STEPHENS, W.E. & DAWSON, J.B. (1977): Statistical comparison between pyroxenes from kimberlite and their associated xenoliths. *J. Geol.* **85**, 433-449.
- WELLS, A.J. (1956): Corundum from Ceylon. *Geol. Mag.* **93**, 25-31.
- WICKS, F.J. & PLANT, A.G. (1979): Electron-microprobe and X-ray-microbeam studies of serpentine textures. *Can. Mineral.* **17**, 785-830.
- _____, WHITTAKER, E.J.W. & ZUSSMAN, J. (1977): An idealized model for serpentine textures after olivine. *Can. Mineral.* **15**, 446-458.

Received October 31, 1984, revised manuscript accepted June 6, 1985.